

Study of Rotating-Wave Electromagnetic Modes for Applications in Space Exploration

Jose E. Velazco*

ABSTRACT. — Rotating waves are circularly polarized electromagnetic wave fields that behave like traveling waves but have discrete resonant frequencies of standing waves. In JPL's Communications Ground Systems Section (333), we are making use of this peculiar type of electromagnetic modes to develop a new generation of devices and instruments for direct applications in space exploration. In this article, we present a straightforward analysis about the phase velocity of these wave modes. A derivation is presented for the azimuthal phase velocity of transverse magnetic rotating modes inside cylindrical cavity resonators. Computer simulations and experimental measurements are also presented that corroborate the theory developed. It is shown that the phase velocity of rotating waves inside cavity resonators increases with radial position within the cavity and decreases when employing higher-order operating modes. The exotic features of rotating modes, once better understood, have the potential to enable the implementation of a plethora of new devices that range from amplifiers and frequency multipliers to electron accelerators and ion thrusters.

I. Introduction

JPL's Communications Ground Systems Section (333) is currently conducting research on several technologies for applications in the Deep Space Network (DSN), Mars exploration, radio astronomy, energy storage, and electric propulsion, among others. Several of these technologies share a common denominator, which is the use of microwave resonators. We are designing microwave cavity resonators that employ circularly polarized electromagnetic modes that we refer to as rotating modes. The rotating modes have the peculiarity that they operate at the frequency ω and that they rotate azimuthally about the device axis with a rotating frequency proportional to ω [1].¹ In one application, we use the rotating feature of these waves to synchronize the rotating wave fields with spinning electrons to produce electron acceleration. The resulting miniature accelerator is being proposed as a new X-ray source for standoff surveying of the Martian landscape. Another application we are developing involves placing solid-state amplifiers in the path of the rotating wave to produce

* Communications Ground Systems Section.

¹ J. E. Velazco, PhD Dissertation, George Mason University, 1994.

The research described in this publication was carried out by the Jet Propulsion Laboratory, California Institute of Technology, under a contract with the National Aeronautics and Space Administration. © 2016 California Institute of Technology. U.S. Government sponsorship acknowledged.

high-power electromagnetic radiation via a novel spatial power combining technique.² This advanced compact power amplifier has direct applications in both radar and communications for ground and flight missions.³ A third application we are pursuing is for electric propulsion wherein rotating waves are used to produce the so-called cyclotron acceleration of ions to generate unparalleled ion thrust and specific impulse. Other applications of these rotating waves include diodeless microwave rectifiers for power beaming, terahertz frequency multipliers, high-power phase array transmitters, super-fast flywheel energy storage devices, microwave motors, etc.

All the new concepts discussed above exploit the gyrating nature of rotating wave modes. This article describes our efforts to better understand the rotational properties of these wave fields. Specifically, we concentrate on analyzing and measuring the phase velocity of rotating modes. In what follows, we calculate the phase velocity of rotating wave fields, present computer simulations of these modes carried out in the code High-Frequency Structure Simulator (HFSS), as well as report on experimental measurements of the phase velocity of the rotating wave fields.

II. Transverse Magnetic TM_{mnp} Modes

In this article, we shall concentrate on discussing transverse magnetic (TM) electromagnetic modes generated inside cylindrical cavity resonators. Specifically, we study the rotational velocity of TM_{mnp} modes with indices m , n , and p that denote, respectively, the azimuthal, radial, and axial wave periodicity. Furthermore, we analyze TM_{mnp} asymmetric modes with $m \geq 1$ to ensure we deal only with rotating modes [1].⁴ Transverse electric (TE) modes can be similarly analyzed.

We shall assume that a cylindrical resonator, with a radius a and length L , holds a transverse-magnetic TM_{mn0} mode with no axial periodicity (i.e., $p = 0$). The complete set of field equations for the TM_{mn0} mode, in cylindrical coordinates (r, ϕ, z) is given by [1]:⁵

$$E_z(r, \phi, z, t) = E_o J_m(k_{\perp} r) \cos(\omega t - m\phi) \quad (1)$$

$$H_r(r, \phi, z, t) = \frac{\omega \epsilon E_o}{k_{\perp}^2} \left(\frac{m}{r} \right) J_m(k_{\perp} r) \cos(\omega t - m\phi) \quad (2)$$

$$H_{\phi}(r, \phi, z, t) = \frac{\omega \epsilon E_o}{k_{\perp}} J'_m(k_{\perp} r) \sin(\omega t - m\phi), \quad (3)$$

where E_o is a field constant and $J_m(k_{\perp} r)$ is the m th-order Bessel function of the first kind. The radial wave number $k_{\perp} = u_{mn}/a$, u_{mn} is the n th zero of $J_m(u)$, and t is the time coordi-

² J. E. Velazco, "Spatial Power Combining Mechanism (SPCM) for the Generation and Amplification of Electromagnetic Radiation," JPL NTR 50016, provisional patent CIT File No.: CIT-7505-P.

³ Ibid.

⁴ J. E. Velazco, PhD Dissertation, George Mason University, 1994.

⁵ Ibid.

nate. The azimuthal index can take values $m = \pm 1, \pm 2, \pm 3, \dots$, ϵ is the permittivity of free space, and [3]

$$J'_m \equiv \left(\frac{d}{dk_{\perp} r} \right) [J_m(k_{\perp} r)] = \left[\frac{m}{k_{\perp} r} J_m(k_{\perp} r) - J_{m+1}(k_{\perp} r) \right].$$

The radian frequency ω for these modes is given by the dispersion relation [5] which, for $p = 0$, is reduced to

$$\frac{\omega}{c} = \frac{u_{mn}}{a}, \quad (4)$$

where $c = (\mu\epsilon)^{-1/2}$ is the speed of light.

Figure 1 shows plots of Bessel functions for $m = 0, 1, 2, 3$ including the location of various zeros of J_m and J'_m . It is of interest to note in the figure the significance of u_{mn} . According to Equation (4), once ω is selected, u_{mn} dictates the value of the cavity radius a . The higher the azimuthal index m , the larger the cavity radius. For example, for $m = 1$, $a \cdot \omega/c = 3.832$; for $m = 2$, $a \cdot \omega/c = 6.380$; for $m = 3$, $a \cdot \omega/c = 6.832$ and so on. If a TM_{m10} mode is selected to operate at $m = 3$ instead of, say, $m = 1$, the cavity radius would almost double in size; that is, $a(\text{TM}_{310})/a(\text{TM}_{110}) = 1.7$.

In order to examine the phase velocity of the rotating wave fields, we hereafter shall concentrate on analyzing the axial electric field, Equation (1). Upon inspection of this rotating

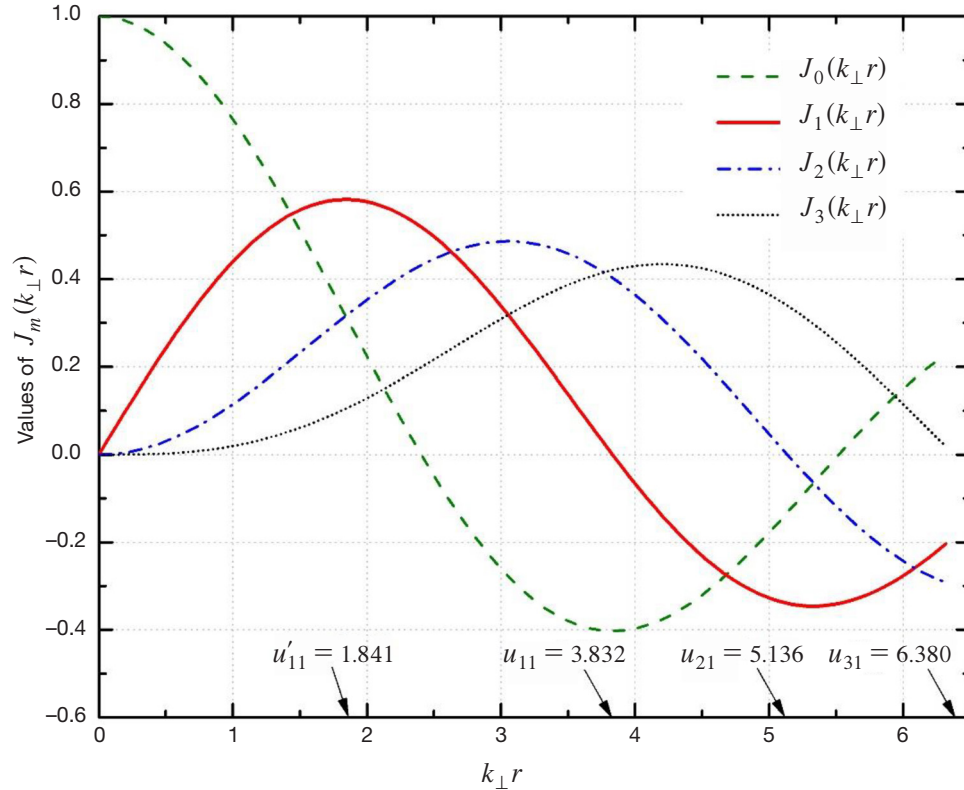


Figure 1. Bessel functions plots for $m = 0, 1, 2, 3$.

wave, we should note that this field resembles a frozen field in space that rotates azimuthally about the cavity axis. At any equiphase spot on the frozen field, the following condition is met:

$$\omega t - m\phi = C, \quad (5)$$

where C is a constant. Applying derivatives to Equation (5) and solving for the rotating frequency $\Omega_r \equiv d\phi/dt$, we obtain

$$\Omega_r \equiv \frac{d\phi}{dt} = \frac{\omega}{m}. \quad (6)$$

At any radial position r , the fields' ϕ -directed phase velocity v_p is given by [4]

$$v_p = \Omega_r \cdot r = \frac{\omega}{m} \cdot r. \quad (7)$$

Equation (7) states that the phase velocity of TM_{mn0} rotating fields increases with the radial coordinate r . The larger the radius, the higher the azimuthal phase velocity of the wave field. For instance, there is a critical radius r_c at which the phase velocity v_p equals the speed of light. That is,

$$v_{p_c} = c = \frac{\omega}{m} \cdot r_c. \quad (8)$$

Solving for r_c and making use of Equation (4), we obtain

$$r_c = \frac{mc}{\omega} = \frac{m}{u_{mn}} a. \quad (9)$$

The critical radius r_c is an important parameter to take into account, especially when dealing with charged particles. It was found in previous work [5] that synchronous interactions between magnetized charged particles and rotating fields inside a resonator were limited to areas with radial positions $r \leq r_c$ wherein the phase velocity is lower or equal than the speed of light.

Furthermore, upon inspection of Equation (1) it can be observed that the rotating electric field inside the resonator peaks (i.e., $J'_m(u)$ achieves a maximum), at a radial value r_p given by

$$r_p = \frac{u'_{mn}}{u_{mn}} \cdot a, \quad (10)$$

while the associated phase velocity measured at r_p is

$$v_{p_p} = \frac{u'_{mn}}{m} \cdot c, \quad (11)$$

where u'_{mn} is the n th root of the $J'_m(u) \equiv \frac{dJ_m(u)}{du} = 0$. Proper selection of u'_{mn} and m so as to minimize $\frac{u'_{mn}}{m}$ should yield phase velocities v_{p_p} near the speed of light. Plots of r_p/a and v_{p_p}/c as a function of m , for various TM_{m10} modes, are shown in Figure 2.

Note in Figure 2 that for larger values of m , (i.e., $m \gg 1$), v_{p_p} approaches the speed of light. Furthermore, it can be observed in the figure that as the azimuthal periodicity is increased

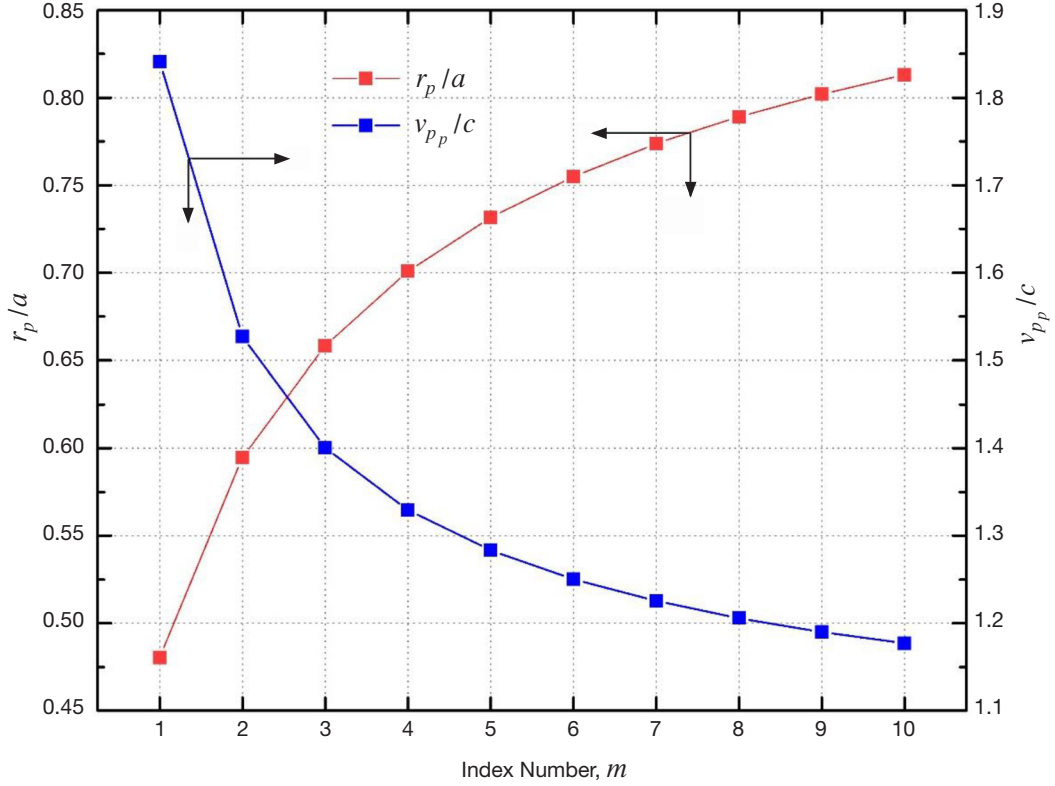


Figure 2. Plots of r_p/a and v_{pp}/c as a function of m are shown for various TM_{m10} modes.

(i.e., a higher-order mode is selected), the radial location of the electric field peak is gradually pushed towards the edge of the cavity wall, $r_p \rightarrow a$.

The flight time it takes the rotating wave to cover a complete revolution about the cavity axis, T_{RW} , is calculated as the ratio of the distance travelled by the wave, $2\pi r$, over its velocity, v_p . That is,

$$T_{RW} = \frac{2\pi r}{v_p} = \frac{2\pi}{\omega} \cdot m. \quad (12)$$

It is noteworthy that the rotational period T_{RW} is independent of the radial coordinate, which means that at any radial position within the cavity resonator the wave takes the same amount of time to complete a revolution about the axis. In addition, the flight time is proportional to the azimuthal periodicity of the wave m . This means that for rotating modes operating with larger values of m , the wave slows down by m [Equation (7)], which results in the wave taking longer to complete a revolution around the cavity.

We are currently taking advantage of these key features of TM_{mn0} rotating modes for the implementation of a new generation of devices and instruments. A judicious selection of the mode index m will allow us to operate rotating modes at a frequency ω while their wave fields rotate at ω/m . Larger values of m slow down the wave, thus increasing their flight time within the cavity.

An illustration of this concept is shown in Figure 3, where the axial electric field of a TM_{310} mode is plotted. In this example, $m = 3$ ($u_{31} = 6.380$ and $u'_{31} = 4.201$), which yields $r_p/a = 0.658$ and $v_{p_p}/c = 1.4$. Note that the wave, having an azimuthal periodicity $m = 3$, features three peaks and three valleys. Moreover, these wave fields resonate at ω but rotate azimuthally about the cavity axis at $\omega/3$. The associated flight time, given by Equation (12), is $T_{RW} = 3 \cdot 2\pi/\omega$ (it takes the wave three radio-frequency periods to complete one revolution).

It should be pointed out that the phase velocity derivations presented here apply to both TE and TM rotating modes inside cylindrical cavity resonators. In the next section, we present a case study for TM modes.

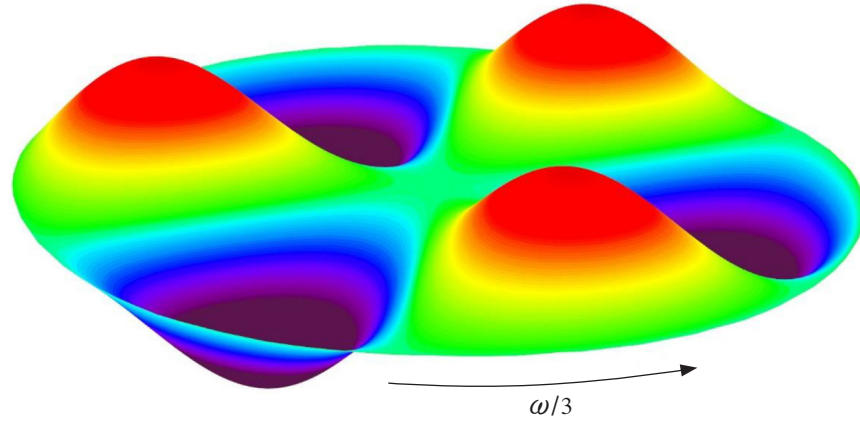


Figure 3. A surface plot of the axial electric field of a TM_{310} rotating mode in a cylindrical resonator. The height of the surface is proportional to E_z . The fields operate at ω but rotate about the axis at $1/3 \omega$.

A. Transverse Magnetic TM_{110} Mode

In this section, we study the TM_{110} rotating mode inside a cylindrical cavity resonator. An expression for the axial electric field for this mode can be deduced from Equation (1) as

$$E_z(r, \phi, z, t) = E_0 J_1(k_{\perp} r) \cos(\omega t - \phi), \quad (13)$$

where the operating frequency ω is given by Equation (4), $k_{\perp} = u_{11}/a$ and $u_{11} = 3.832$. The fields of this mode both oscillate and rotate azimuthally at the same frequency ω [1]. Figure 4(a) shows the field lines of the TM_{110} rotating mode inside a cylindrical cavity. The electric field lines go in and out of the picture and peak at a radius $r_p = \frac{u'_{11}}{u_{11}} \cdot a = \frac{1.841}{3.832} \cdot a = 0.48 \cdot a$. In Figure 4(b), we show a surface plot of the axial electric field E_z obtained with Equation (13).

In order to corroborate the phase velocity calculations shown above, we performed HFSS computer simulations and experimental studies of the TM_{110} rotating mode inside a cavity resonator. The cavity is cylindrical in geometry and is designed to operate at 2.4 GHz. Per Equation (4), the cavity radius is $a = 7.5$ cm whereas the cavity length, being frequency independent, is arbitrarily set to $L = 5$ cm. We used four test ports located at positions A,

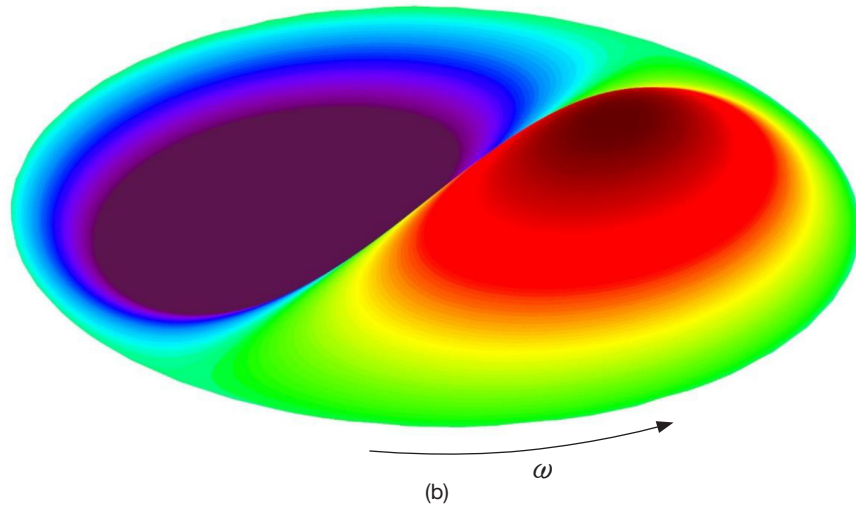
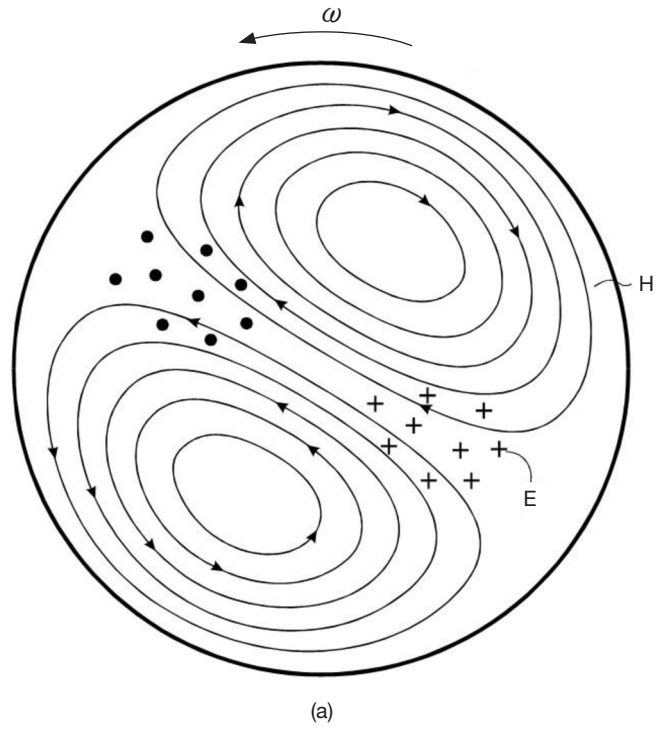


Figure 4. (a) Electromagnetic field lines and (b) surface plot of axial electric field E_z for TM_{110} rotating mode.

B, C, and D, as shown in Figure 5. The radial position of each port is $r_p = 3.75$ cm and the azimuthal angle between neighboring ports is 90 deg. The goal of these studies was to measure the azimuthal phase velocity of the E_z field by measuring the time τ it would take the rotating wave to move from point A to B, B to C, and C to D, respectively. Per Equation (12), the rotating wave travels one complete revolution (from 0 to 2π) in one RF period ($T_{RW} = 2\pi/\omega$). Therefore, the flight time between two neighboring test ports, $\pi/2$ apart, should be equal to a quarter of an RF period, that is:

$$\tau_{A-B} = \tau_{B-C} = \tau_{C-D} = \frac{\pi}{2\omega}. \quad (14)$$

In the next section, we present HFSS simulations performed to verify the accuracy of Equation (14).

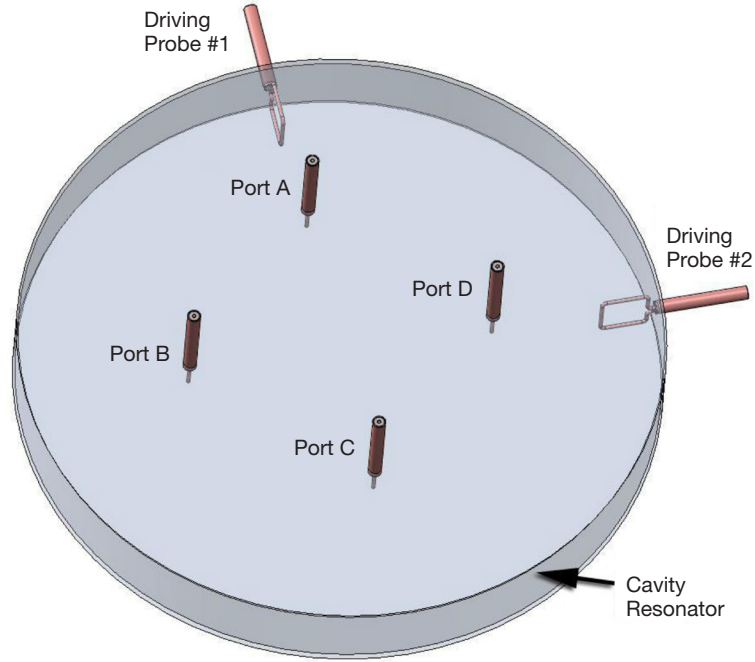


Figure 5. Cylindrical microwave cavity showing the location of the various driving and test ports.

B. HFSS Computer Simulations

We input the cavity geometry ($a = 7.5$ cm, $L = 5$ cm) into the HFSS code to generate the TM_{110} rotating mode and to study the phase velocity of the wave fields. The TM_{110} rotating mode was launched in HFSS via two driving ports placed at $r = a = 7.5$ cm, 90 deg apart azimuthally, working at a frequency of 2.4 GHz (see Figure 5). In addition, a time shift of 90 deg was also provided between the two driving signals. The driving probes are two 50-ohm coaxial lines each terminated in a magnetic loop. Figure 6 shows an HFSS contour plot of the axial electric field along the cavity cross-section ($r - \phi$). Note that this plot correctly represents the TM_{110} mode axial electric field denoted by Equation (13), featuring a peak and a valley as one moves azimuthally from 0 to 2π .

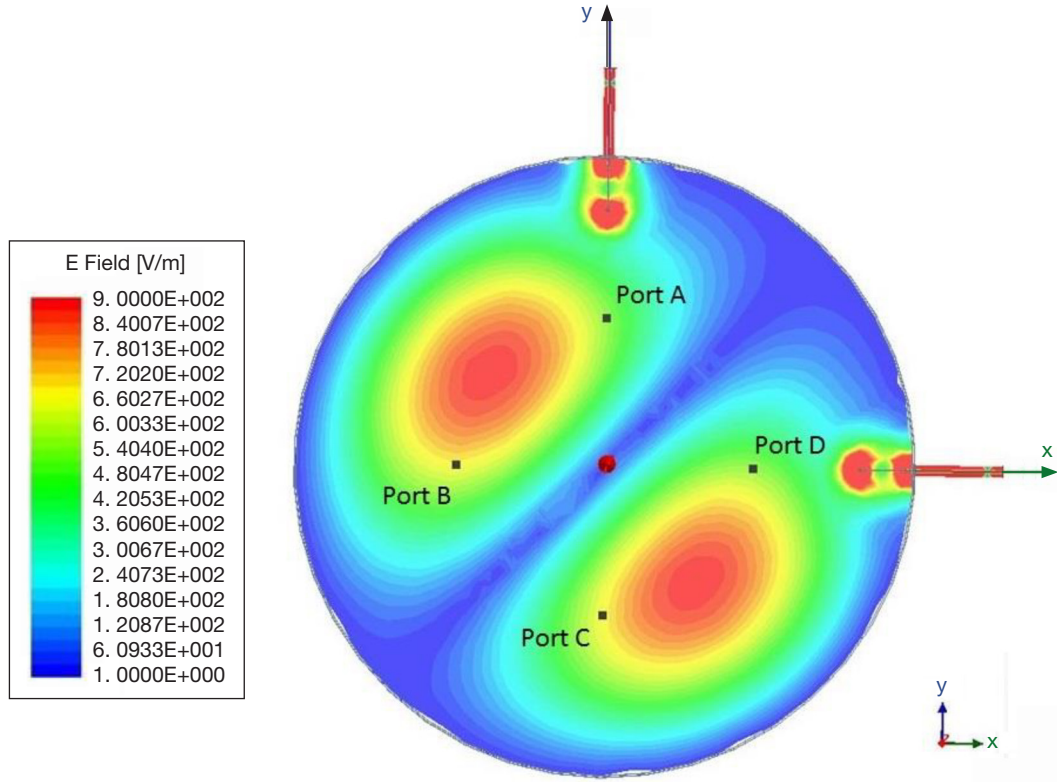


Figure 6. HFSS-calculated contour plot of the axial electric field E_z of the TM_{110} . Note that this plot illustrates the intensity of the field (field polarity is not shown). The red-colored areas denote the peak of the electric field.

In Figure 7, we show four snapshots of the axial electric field E_z taken with a difference of a quarter of an RF period between them. Note that in going from $\phi = 0$ to $\phi = 270$ deg, as expected, the mode rotates counterclockwise about the cavity axis. We also measured the RF electric field at the four test points A–D, respectively, shown in Figure 5. The four test points are located at $r = r_p = 3.75$ cm. Plots of the electric field measured along these points as a function of phase angle of the driving signals are shown in Figure 8. Noteworthy is the fact that each trace is delayed with respect to the previous one by $\phi = 90$ deg. For example, in moving from A to B, the wave takes a quarter of an RF period, $\phi = 90$ deg, or $\pi/(2\omega)$, as predicted by Equation (14). The same results are obtained between points B and C, and C and D, respectively, as shown in the additional traces. The results obtained in HFSS confirm the theoretical phase velocity analysis described earlier.

To conclude with the phase velocity analysis of TM_{110} rotating modes, we also performed experimental measurements of the mode dynamics inside a resonator. Results of these measurements are presented next.

C. Experimental Measurement of Phase Velocity

The purpose of these final studies was to experimentally verify Equations (7), (12), and (14). We built a cylindrical resonator for operation in the TM_{110} mode at a frequency of 2.4 GHz. The cavity radius is $a = 7.5$ cm and the cavity length was set to $L = 5$ cm. The RF signal is provided by a Hewlett Packard (HP) 8350B signal generator furnished with an 83555A

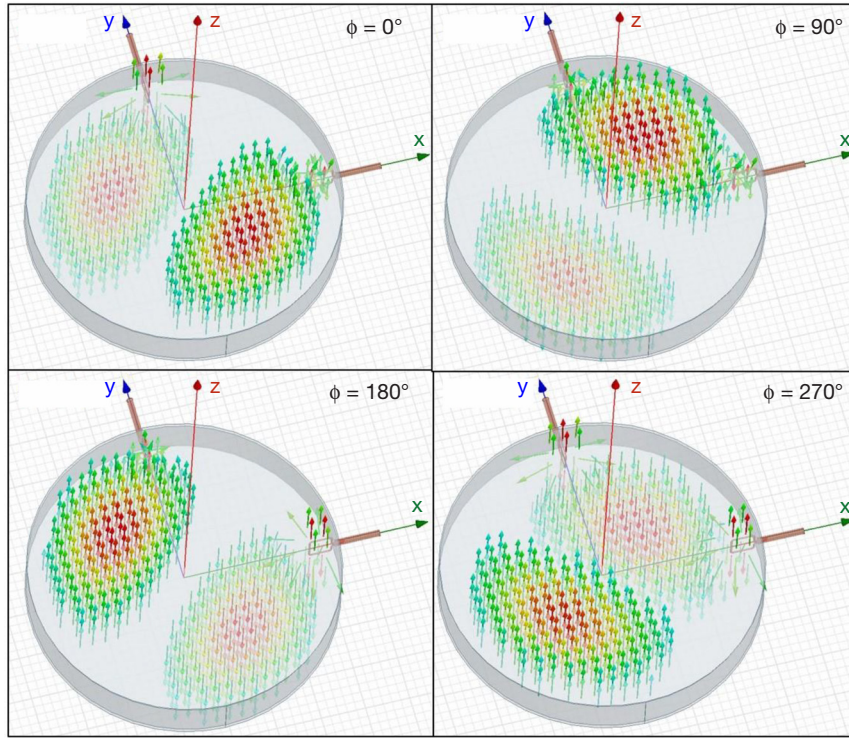


Figure 7. Vector plots of the axial electric field E_z of the TM_{110} mode obtained in HFSS. Plots are taken with a difference of a quarter of an RF period (90 deg) between them. Note that the wave rotates counterclockwise about the cavity axis.

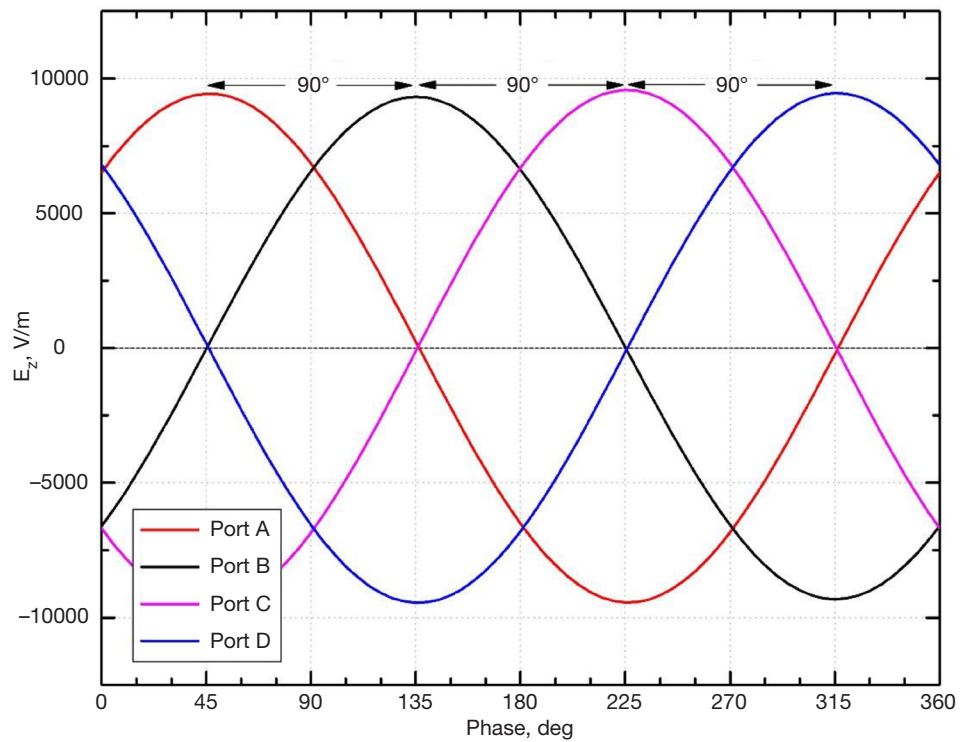


Figure 8. Time history of the axial electric field E_z measured along the test ports A–D obtained in HFSS.

plugin. We used two driving probes to generate the rotating mode inside the cavity [6]. The driving probes were placed around the edge of the cavity ($r = a$) and 90 deg apart azimuthally. A 90-deg time shift was also applied between the driving probes via a 90-deg hybrid in order to successfully generate the rotating mode [6]. We included four test ports located at the radial position $r_p = 2.75$ cm and 90 deg apart from each other. Figure 9 shows a picture of the cavity resonator illustrating the position of the driving ports as well as the test ports, which are labeled as A, B, C, and D, respectively.

For the purpose of measuring the rotating wave dynamics, we used coaxial capacitive probes in each port that were critically coupled to the cavity to measure the electric rotating wave field at that point. The output of each port was directly connected to an 8-GHz 25 GS/s Tektronix DSA70804B oscilloscope via suitable coaxial lines.

At this point, it is convenient to describe the expected wave dynamics along the area where the test ports are positioned. Recall that the wave resembles a frozen field featuring a peak and a valley [as shown in Figure 4(b)] that spins about the cavity axis. As the rotating wave travels azimuthally, it scans over each of the electric probes, completing a 360-deg revolution in one RF period. Consequently, as the wave moves over a specific probe, the probe will sense the peaks and valleys of the rotating field passing over it, causing the signal measured by that probe to be sinusoidal. In Figure 10 we show a typical oscilloscope measurement of the RF electric field obtained at port A. Note that, as expected, the measured signal is sinusoidal with a period of 417 ps (corresponding to a frequency of 2.4 GHz).

We next measured ports A and B on the oscilloscope. The time it takes the wave to travel from A to B is equal to the arc travelled by the wave divided by the wave velocity. Figure 11 shows a typical result of the simultaneous measurements at ports A and B. Note that the signal from port B is delayed with respect to port A by 104 ps, which is exactly a quarter of an RF period. This delay results from the wave taking that time to move from A to B. The wave's phase velocity between point A and B can then be calculated as $\frac{1}{4}(2\pi \cdot 2.75 \cdot 10^{-2}) / (104 \cdot 10^{-12}) = 5.52 \cdot 10^8$ m/s, which turns out to be $1.84 \cdot c$. These results corroborate our theory [Equation (11)] that the rotating wave at a radial position r_p is travelling at u'_{11} times the speed of light (where $u'_{11} = 1.841$). Figure 12 shows the four signals measured simultaneously from ports A thru D, respectively. Again, one can observe that in travelling from A to B, B to C, and C to D, the rotating wave takes exactly a quarter of a period (104 ps), as predicted earlier.

We should also note that if the mode launched inside the cavity is not a rotating mode (e.g., a standing-wave mode instead), the signals measured by the oscilloscope would be superimposed and will depict different amplitudes. Figure 13 shows oscilloscope measurements from ports A–D when a standing wave mode is launched inside the cavity resonator via driving probe number two. Note that, indeed, the signals have different amplitudes and are superimposed, as described in previous lines.

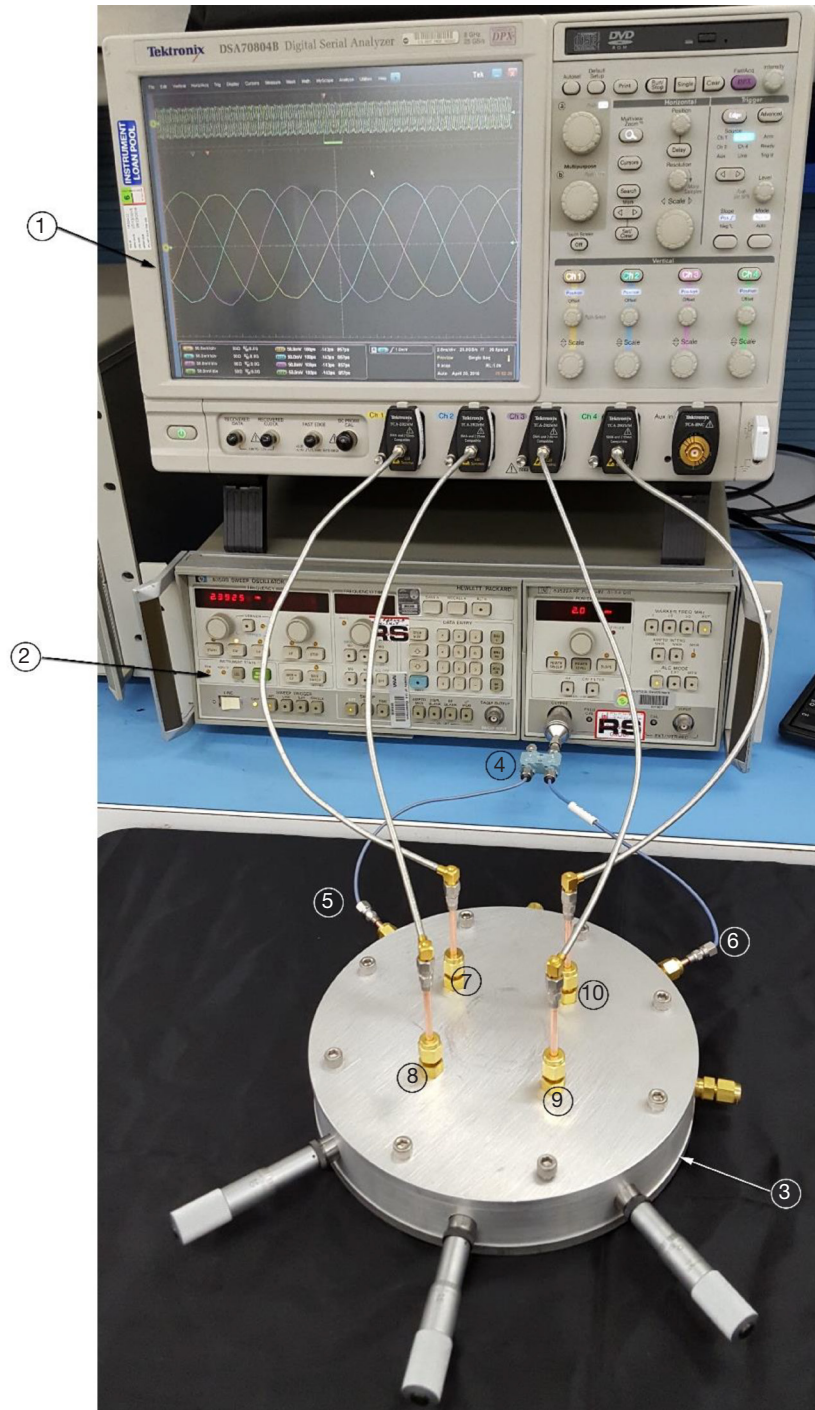


Figure 9. Picture of experimental apparatus and microwave resonator designed to operate at 2.4 GHz in the TM_{110} mode. Shown are: ① 25 GS/s oscilloscope; ② HP signal generator; ③ S-band microwave resonator; ④ 90-deg hybrid; ⑤, ⑥ driving probes; ⑦ port A; ⑧ port B; ⑨ port C; and ⑩ port D.

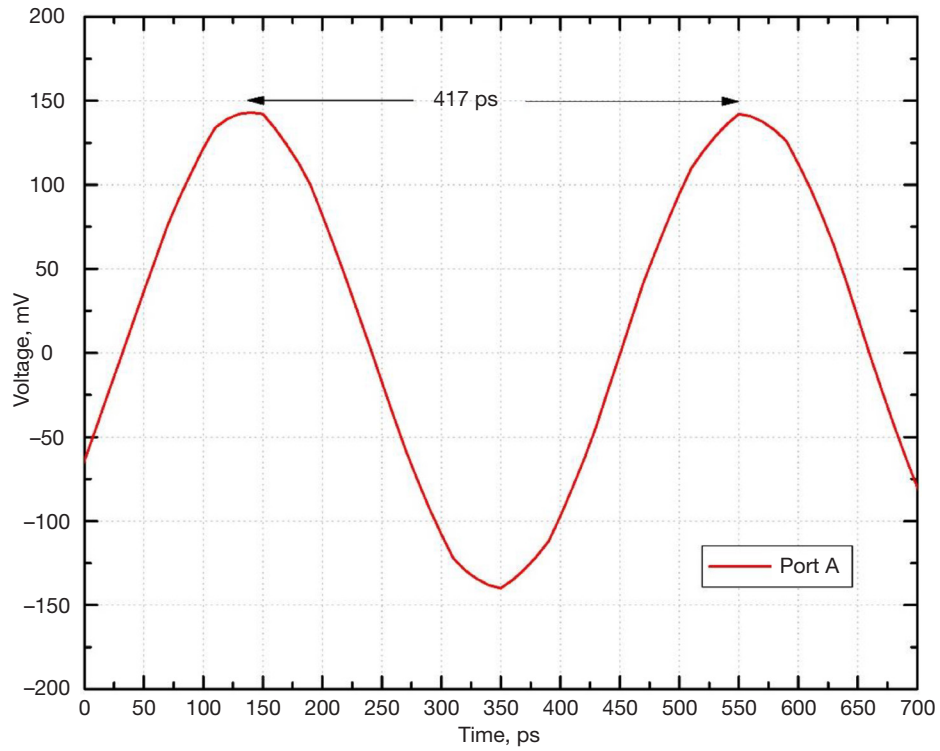


Figure 10. Oscilloscope trace obtained from port A. Note that the sinusoidal signal has a period of 417 ps, which corresponds to the operational frequency of 2.4 GHz.

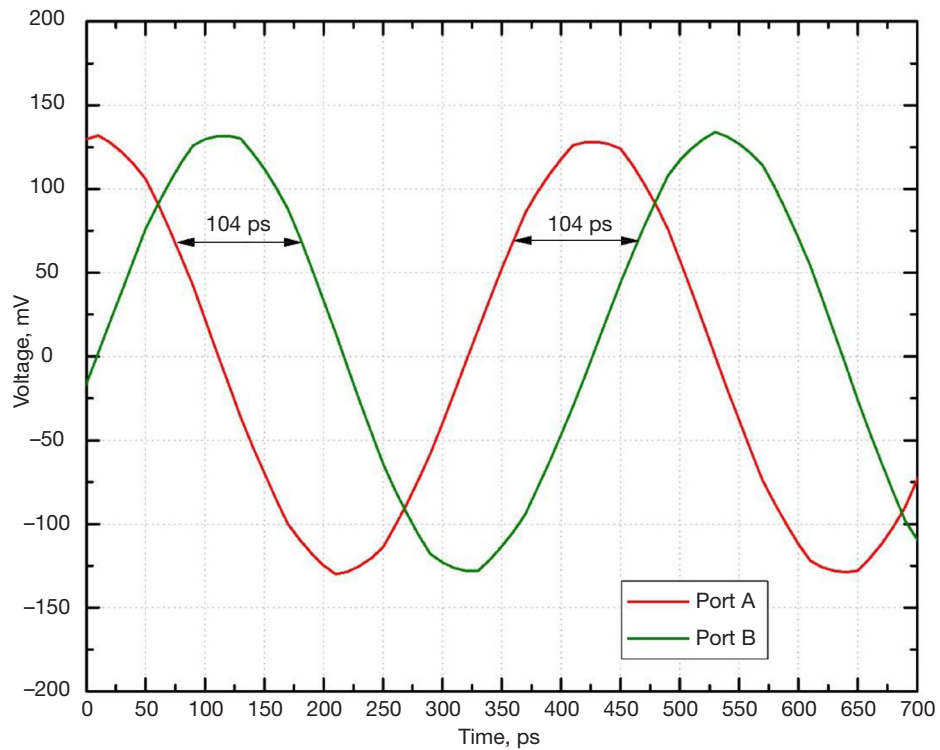


Figure 11. Oscilloscope traces obtained simultaneously from port A and port B. The delay between the two traces is 104 ps, corresponding to a quarter of an RF period.

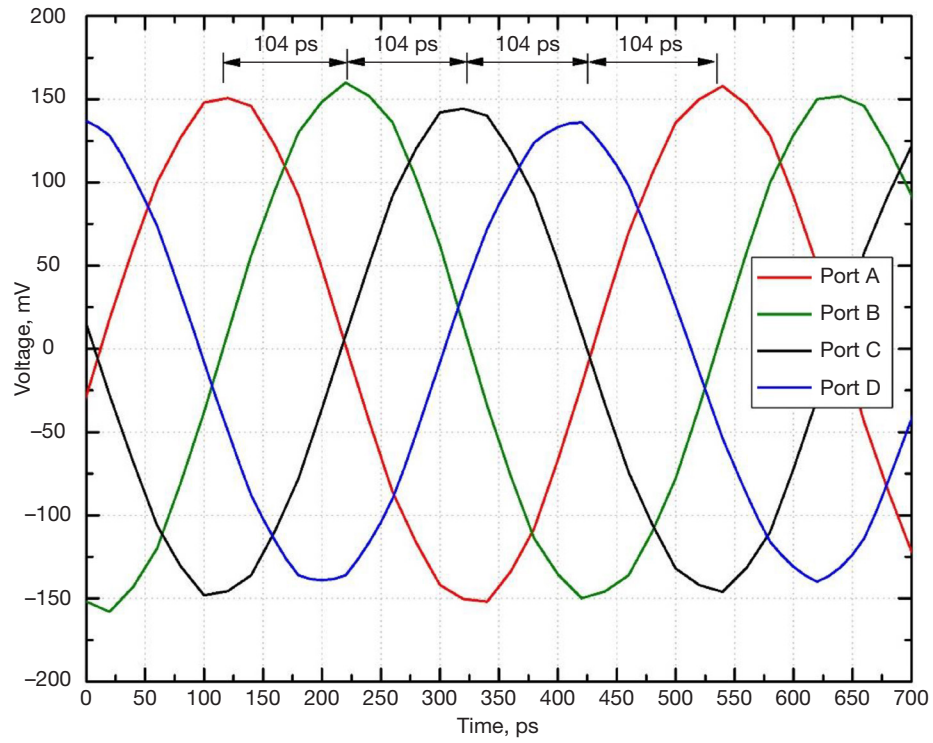


Figure 12. Shown are four oscilloscope traces obtained simultaneously from port A, B, C, and D, respectively. Note that the delay between two consecutive ports is 104 ps.

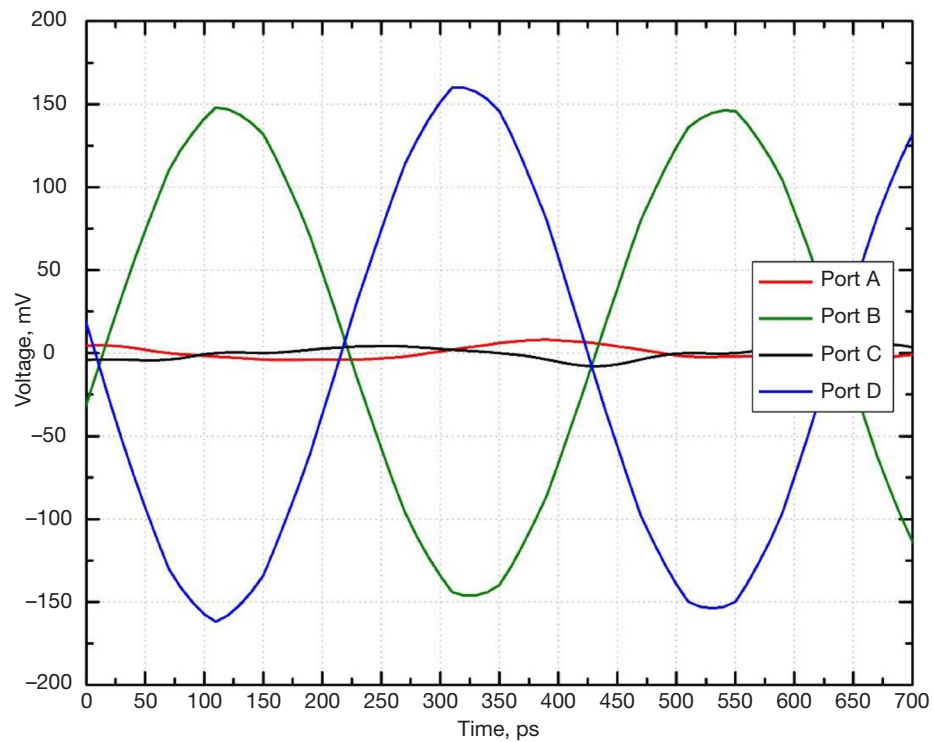


Figure 13. Oscilloscope traces obtained simultaneously from port A, B, C, and D, when a standing-wave mode is launched inside the cavity.

III. Conclusions

We have presented a basic theoretical analysis for the phase velocity of TM_{mn0} rotating modes inside cylindrical resonators. It was shown that rotating waves slow down as the azimuthal index m of the wave is made larger. Furthermore, it was also found that the ϕ -directed velocity increases as the radial coordinate is increased. Expressions were derived for calculating the radius at which the electric field peaks within the cavity and the corresponding velocity, at that radius. We found agreement among theory, simulations, and experimental testing.

These initial results are a prelude to further research being conducted in the JPL Communications Ground Systems Section (333) on rotating modes. We plan to perform further studies about energy and power carried by rotating waves as well as rotating wave field analysis near the cavity axis, e.g., $k_{\perp} r \ll 1$. Our findings will be reported in a timely manner.

Additionally, it should be stated that the section is actively pursuing the development of an advanced spatial power combiner amplifier (SPCA)⁶ that uses the rotating mode features described herein.

We believe that the rotating modes studied here have great potential to be a technology enabler for a new breed of devices and instruments for space exploration, the military, and industry.

Acknowledgments

Thanks to Mark Taylor of JPL (Section 333) for his help with the HFSS simulations, testing of the cavity resonator, and data plotting; Steven Montanez of JPL (Section 333) for fabricating the cavity probes; and Michael Young of JPL (Section 333) for machining the cavity resonator.

⁶ J. E. Velazco, "Spatial Power Combining Mechanism (SPCM) for the Generation and Amplification of Electromagnetic Radiation," JPL NTR 50016, provisional patent CIT File No.: CIT-7505-P.

References

- [1] J. E. Velazco and P. H. Ceperley, "A Discussion of Rotating Wave Fields for Microwave Applications," *IEEE Transactions on Microwave Theory and Techniques*, vol. 41, no. 2, pp. 330–335, MTT-41, February 1993.
- [2] M. Abramowitz and I. A. Stegun, *Handbook of Mathematical Functions*, New York: Dover, pp. 358, 361, 437, 1964.
- [3] S. Liao, *Microwave Devices and Circuits*, Englewood Cliffs, New Jersey: Prentice-Hall, pp. 137–138, 1985.
- [4] J. R. Pierce, *Almost All About Waves*, Cambridge, Massachusetts: Massachusetts Institute of Technology, p. 88, 1974.
- [5] J. E. Velazco and F. M. Mako, "Limited Spatial Region for Synchronous Beam-Wave Interactions," *Applied Physics Letters*, vol. 63, no. 22, pp. 3087–3089, November 29, 1993.
- [6] P. H. Ceperley and J. E. Velazco, "Tuning a Rotating Mode Resonator," *Review of Scientific Instruments*, vol. 66, no. 1, pp. 256–260, January 1995.